The Hydrogel Nature of Mammalian Cytoplasm Contributes to Osmosensing and Extracellular pH Sensing

Johannes Fels,[†§] Sergei N. Orlov,[†‡] and Ryszard Grygorczyk[†‡*]
[†]Research Centre, Centre hospitalier de l'Université de Montréal (CHUM), Hôtel-Dieu, and [‡]Department of Medicine, Université de Montréal, Montréal, Québec, Canada; and [§]Institute of Physiology II, University of Münster, Münster, Germany

ABSTRACT Cytoplasm is thought to have many hydrogel-like characteristics, including the ability to absorb large amounts of water and change volume in response to alterations in external environment, as well as having limited leakage of ions and proteins. Some gel-like behaviors have not been rigorously confirmed in mammalian cells, and others should be examined under conditions where gel volume can be accurately monitored. Thus, possible contributions of cytoplasm hydrogel properties to cellular processes such as volume sensing and regulation remain unclear. We used three-dimensional imaging to measure volume of single substrate-attached cells after permeabilization of their plasma membrane. Permeabilized cells swelled or shrinked reversibly in response to variations of external osmolality. Volume changes were 3.7-fold greater than observed with intact cells, consistent with cytoplasm's high water-absorbing capacity. Volume was maximal at neutral pH and shrunk at acidic or alkaline pH, consistent with pH-dependent changes of protein charge density and repulsive forces within cellular matrix. Volume shrunk with increased Mg^{2+} concentration, as expected for increased charge screening and ionic crosslinking effects. Findings demonstrate that mammalian cytoplasm resembles hydrogel and functions as a highly sensitive osmosensor and extracellular pH sensor. Its high water-absorbing capacity may allow rapid modulation of local fluidity, macromolecular crowding, and activity of intracellular environment.

INTRODUCTION

The plasma membrane plays a prominent role in controlling cell volume responses to extracellular and intracellular environment changes. Besides serving as a diffusion barrier that prevents uncontrolled leakage of cellular content, its array of specialized transporters actively regulate electrochemical gradients of inorganic and organic osmolytes between the cell's interior and surrounding medium. Although the role of the plasma membrane in volume-regulatory mechanisms has been widely appreciated, the membrane-enclosed cytoplasm is usually considered a simple aqueous solution in which water and small ions are free to diffuse. Such a paradigm, however, has been extrapolated from studies of dilute solutions and founded on several implicit assumptions that may not be valid in a protein-crowded intact cell milieu (1,2). Cytoplasm consists of a water-containing matrix formed by a cytoskeletal network of interconnected protein fibers that might be better described as an aqueous gel (1,3,4). As such, cytoplasm may have properties similar to hydrogels, a synthetic or natural water-swollen polymeric network containing chemical or physical crosslinks (5). Hydrogels are either neutral or ionic with porous or nonporous structures that can absorb large amounts of water, but the extent of their swelling depends on external osmolality, temperature, and ionic strength. Ability to swell is a major property of artificial and biological gels and is attributed to volume exclusion effect (6), but gels that have a net nondiffusible charge on their insoluble matrix (polyelectrolyte gels) will swell in aqueous media through internal electrostatic repulsion forces between neighboring matrix charges. These repulsive forces are partly screened by mobile counterions in the aqueous medium penetrating the matrix, and their distribution between the gel and the outer solution is determined by the Donnan equilibrium (7–9). Therefore, hydrogel swelling will depend on the ionic composition of the external solution and charge density on the polymeric network, which for biological protein-based hydrogels could be modulated by pH. Multivalent counterions such as Mg^{2+} may have particularly strong effects on gel volume, not only by more efficient charge screening but also due to ionic crosslinking effect, which involves electrostatic attractive forces between multivalent cation and two or more neighboring anionic polymers. Polyelectrolyte gels are intrinsically unstable and would swell indefinitely in the absence of stabilizing forces such as chemical crosslinking of the network; physical forces due to entanglement of the fibrilar elements of the gel; external osmotic pressure; and in biological tissues, physical forces exerted by the extracellular matrix. Another biologically important volume-stabilizing mechanism involves lowering intracellular osmotic pressure by metabolically driven ion pumping out of the cell, which is believed to be responsible for volume stabilization in most intracellular gels (9). Thus, removal or permeabilization of plasma membrane will abolish this volume-stabilizing mechanism and lead to cell swelling due to ion movement driven by the Donnan effect. Indeed, squid axoplasm, after extrusion from the giant axon directly into an artificial axoplasm solution, retains its cylindrical shape and shows significant swelling that is likely a direct manifestation of cytoplasm

Submitted May 19, 2008, and accepted for publication February 17, 2009.

*Correspondence: ryszard.grygorczyk@umontreal.ca

Editor: Elliot L. Elson.

0006-3495/09/05/4276/10 $2.00

doi: 10.1016/j.bpj.2009.02.038

gel-like nature (10). Similar behavior is demonstrated by the intracellular membrane-enclosed insoluble matrix of the secretory granules, which rapidly swells when the interior of the granule is exposed to Ringer's solution. The matrix volume also reversibly shrinks and swells like an ion-exchange gel by changing the valency of cation in the external bathing solution (11). Other gel-like behaviors of the cytoplasm have been observed with whole tissue preparations such as detergent-permeabilized or cut open lens fibers and skinned muscle fiber cells. These preparations show ability to retain large amounts of water, >3 g H_2O/g dry mass (12,13) and limited leakage of ions and proteins (12,14). Retention of water, proteins, and potassium was also observed with isolated permeabilized epithelial cells (15) and lymphocytes (16), consistent with the gel-like nature of cytoplasm. Other examples of biological gels include supracellular gels formed by mucins, which cover and protect epithelial cells in the respiratory, gastrointestinal, and other systems; amphibian epidermis; and the gills in fishes (17). Mucins are tightly packed in acidic intracellular granules containing high milimolar $CaCl_2$ levels and show significant swelling upon exocytotic secretion, consistent with their ability to retain large amounts of water (18). Cytoplasm gel-like hydration properties have also been predicted from studies of model systems such as protein-containing dialysis cassettes (19) and studies with nonliving artificial and natural gels (7,20). Despite much evidence of cytoplasm's gel-like behavior, these properties have not been explicitly incorporated into current models of cell-volume regulation. This is likely because the gel properties of mammalian cytoplasm have been difficult to study at the single-cell level and their contribution to intact cell-volume responses cannot be directly evaluated. This requires testing single-cell cytoplasm behavior under conditions in which its gel-like structure is preserved and volume can be accurately monitored.

In this study, we tested the hypothesis that mammalian cytoplasm is a hydrogel and examined its volume response to external environment changes. We used a three-dimensional (3D) imaging technique developed in our laboratory that allows monitoring volume of single substrate-attached cells after permeabilization of their plasma membrane.

METHODS

Cell-volume evaluation

Cells grown on glass coverslips were mounted in a custom-made flow-through imaging chamber perfused with 37°C solution. To evaluate volume changes of substrate-attached cells, we deployed an upgraded version of the 3D imaging technique described in our previous work (21,22). Briefly, the method involves 3D reconstruction of cell shape based on cell images acquired in two perpendicular directions. Side-view and top-view cell images were acquired with two independent miniature charged-coupled device cameras (Moticam 350, Motic Instruments, Richmond, British Columbia, Canada) and Motic software at 10- to 60-s intervals to closely follow rapid volume changes. 3D topography of the cell surface was reconstructed by a dual image surface reconstruction technique (21). This generated a set of topographical curves of the cell surface from its digitized side-view profile and base outline. Cell volume and surface were calculated from this reconstructed cell topographical model. All calculations were carried out with MATLAB (The MathWorks, Natick, MA). In this study, data plots show relative volume normalized to volume of intact cell in physiological solution.

Solutions

Physiological isotonic solution (PS) contained (in mM): 140 NaCl, 5 KCl, 1 $MgCl_2$, 1 $CaCl_2$, 10 glucose, and 10 HEPES (pH 7.4, adjusted with NaOH). Intracellular-like solution (ILS) contained (in mM): 10 NaCl, 110 KCl, 5 $MgCl_2$, 1 Na-ATP, 1 EGTA, 10 HEPES, 11 DTT, and 25 imidazole (pH 7.4, adjusted with KOH). Osmolality of the solutions was measured with a freezing point osmometer (Advanced Micro Osmometer Model 3300, Advanced Instruments, Norwood, MA) and were 292 ± 3 mOsm for PS and 279 ± 2 mOsm for ILS. Hypertonic solutions were made by addition of mannitol (200 mM, 300 mM, and 400 mM), whereas hypotonic solutions were made by reducing salt (NaCl, KCl) concentration. High Mg^{2+} ILS was prepared by isoosmotic replacement of KCl by $MgCl_2$.

Cells

Culture of human lung carcinoma A549 cells and human bronchial epithelial 16HBE14o$^-$ cells, a gift from Dr. D. Gruenert (California Pacific Medical Center Research Institute), is described in (23). HL-60 cells were cultured in suspension in RPMI containing 10% FBS, 2 mM L-glutamine, 56 U ml^{-1} penicillin G, and 56 μg ml^{-1} streptomycin. Before the experiment, HL-60 cells were treated with phorbol ester (0.1 μM, 24 h) to induce their differentiation and attachment to the glass substrate. All constituents of the culture media were from Invitrogen (Burlington, Ontario, Canada). Cell volume was quantified from cells plated at low density on 22 × 22-mm glass coverslips.

Plasma membrane permeabilization

Except in initial experiments where higher detergent concentrations and longer treatment times were used, the cell plasma membrane in most experiments was permeabilized by brief ~2-min exposure to 5 μg ml^{-1} (~4 μM) of digitonin (Sigma-Aldrich Canada, Oakville, Ontario, Canada) in ILS, followed by washing with digitonin-free ILS. As verified by Trypan Blue staining, ~90% of A549 cells were permeabilized by such treatment. In separate experiments, we found that by adding Trypan Blue at different time points after digitonin treatment,~70% of cells remained permeabilized for at least 30 min, long enough to study their properties. Because some cells resealed their plasma membrane during the 30–40 min period, Trypan Blue staining was always performed at the end of each experiment to verify that the plasma membrane of any given cell under investigation remained permeabilized throughout the entire experiment. Cells that failed this test were rejected from analysis. For comparison, in some experiments, cells were permeabilized with amphotericin B (7.5 μg ml^{-1}, 8 min), which produced essentially the same results as digitonin.

Intracellular pH measurements

Intracellular pH was monitored using a pH-sensitive fluorescent dye BCECF (Invitrogen-Molecular Probes, Burlington, Ontario, Canada). To load cells with the dye, they were incubated (1 h, room temperature) in PS containing 10 μM BCECF-AM, 0.02% Pluronic® F127, and 2.5 mM probenecid. For fluorescence imaging, a coverslip with cells was mounted in an imaging/perfusion chamber attached to a heated platform (P-5, Warner Instruments, Hamden, CT) on the stage of an inverted microscope TE300 (Nikon, Montreal, Quebec, Canada). Details of the fluorescence imaging system are described in our previous work (24).

RESULTS

We hypothesized that mammalian cytoplasm behaves as a hydrogel, and, therefore, its volume should reversibly respond

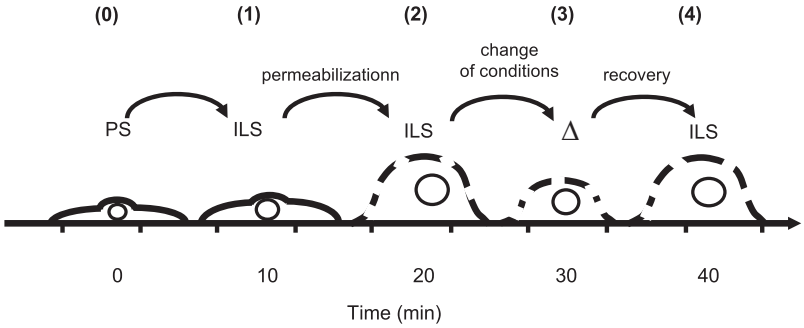

FIGURE 1 Flow-chart of a typical experiment. Cells were mounted in the perfusion chamber and equilibrated in PS (37°C, ~10 min) (*O*); perfusion with ILS (*1*); permeabilization with digitonin (2 min) or amphotericin B (8 min) followed by the wash out (*2*); change of osmolality, pH, or [Mg^{2+}] of the external solution (*3*); return to initial conditions to test reversibility of the volume changes (*4*). Trypan Blue added at this point to verify that the cell remained permanently permeabilized.

to alterations of osmolality, pH, and concentration of divalent cations such as Mg^{2+} in bathing solution.

Plasma membrane permeabilization induces cytoplasm swelling

To gain direct access to the cytoplasm, cell-surface membrane was perforated with a detergent. Because membrane permeabilization is usually associated with cell swelling, we questioned what experimental conditions were required to reproducibly observe such swelling and whether permeabilized cells after initial swelling could attain a stable volume. Fig. 1 shows a flow chart of a typical permeabilization experiment. Glass coverslips with adherent cells were mounted in the side-viewing experimental chamber and cells were perfused with warm (37°C) PS for 10–15 min. During off-line analysis, the volume of a resting intact cell was determined at the end of this equilibration period and used as a reference for the entire experiment. In absolute numbers, volume of intact A549 cells was 2.4 ± 1 pl (1 pl = 1000 μm^3, $n = 50$), which agrees with previously reported values (22). When perfusate was changed to ILS, it resulted in moderate cell swelling of 1.35- ± 0.01-fold initial volume. Volume increase is likely due to depolarization of membrane electrical potential and increased concentration of intracellular Cl^- under high K^+ conditions (see Fig. 2, *a* and *b*) (25) and, in

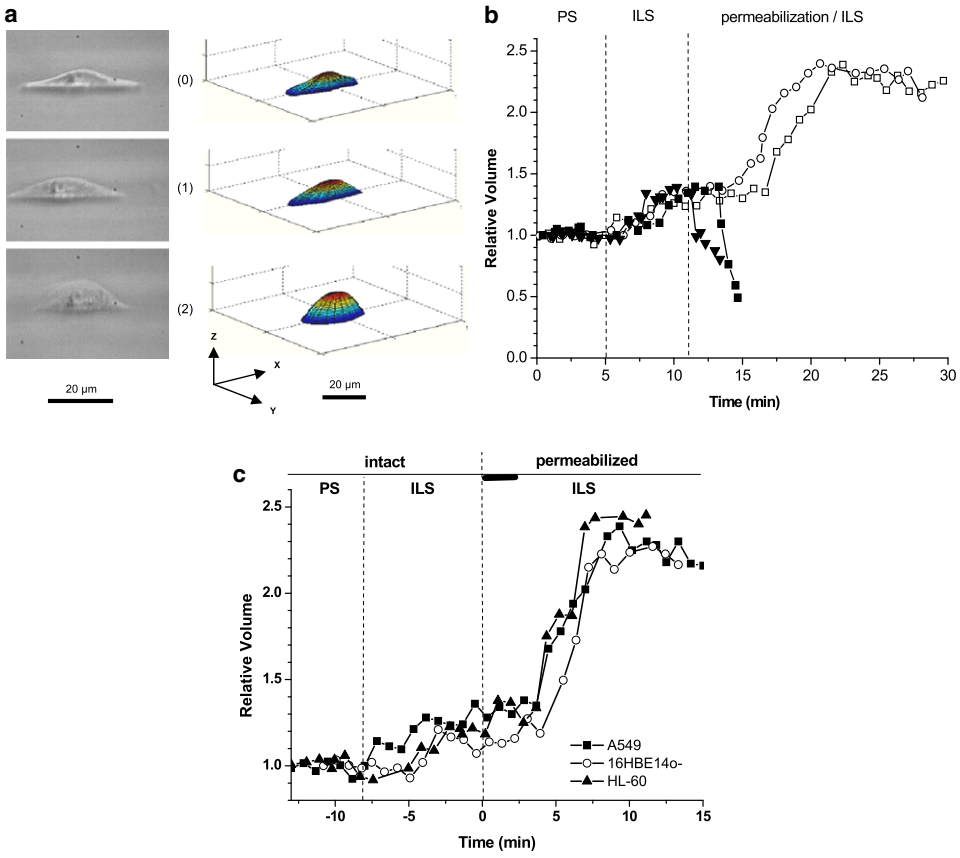

FIGURE 2 (*a*) Light microscopic side-view images of an intact substrate-attached A549 cell in PS (*0*), ILS (*1*), and after plasma permeabilization with digitonin (*2*). The corresponding perspective view of 3D cell models reconstructed by dual image surface reconstruction technique (as described in Methods) is shown on the right, from which absolute cell volume (in pl) was determined. (*b*) Permeabilization-induced relative cell volume changes. Initial absolute cell volume measured in PS ($t = 0$–5 min) was set to 1. When PS was changed to ILS, cells swelled to 1.35- ± 0.01-fold initial volume. After equilibration at $t = 12$ min, cells were permeabilized with 25 μg/ml digitonin (■) or 0.1% Triton X-100 (▼), which remained in the perfusate throughout the experiment. In another series of experiments, cells were permeabilized with 5 μg/ml digitonin for 2 min (□) or amphotericin B (7.5 μM, 8 min, ○). The detergent was washed away afterward with ILS. Representative traces are shown for $n = 5$ (amphotericin B) to $n = 50$ (digitonin). (*c*) Comparison of membrane permeabilization-induced swelling of three different cell lines A549 (■), 16HBE14o$^-$ (○), and HL-60 (▲). Representative traces are shown for $n = 50$ (A549 cells) and $n = 4$ for two other cell lines. The thick horizontal bar indicates a 2 min period of digitonin application.

part, due to slightly lower (~4%) osmolality of the ILS compared to PS. After cell volume reached a new stable level, cell plasma membrane was permeabilized by continuous perfusion with ILS containing digitonin. As Fig. 2 *b* reveals, after plasma membrane permeabilization with 25 μg/ml digitonin, a typical concentration used for permeabilizing many cell types, cells rapidly collapsed loosing most of their intracellular content. Similar results were obtained with Triton X-100, which even at the lowest concentration tested (0.1%) led to rapid solubilization of cell membrane and cytoplasm, resulting in the collapse of cellular structure. In some experiments with lower digitonin concentration (10 μg/ml), a transient swelling was observed followed by cell collapse, suggesting that cell swelling could be observed. However, permeabilization procedure with such high detergent concentration leads to destruction of cytoplasm structural integrity and leakage of cellular content. To avoid this, we used 5 μg/ml digitonin and shortened the treatment time to ~2 min. With this permeabilization protocol, different behavior of A549 cells was observed; they swelled 2.2-fold reaching a steady level within ~5 min. The same result was observed when another detergent, amphotericin B (7.5 μg/ml, 8 min) was used. Similar swelling was observed with human bronchial epithelial 16HBE14o$^-$ and HL-60 leukemia cells, demonstrating that the effect is not unique to A549 cells (see Fig. 2 *c*). This swelling is attributable to the Donnan effect and is a direct result of abolishing the volume-stabilizing function of the plasma membrane. The fact that after initial swelling, permeabilized cells attained a stable volume indicates a limited leakage of cellular proteins. Volume of permeabilized cells in these experiments remained stable for at least 30 min, allowing investigating their responses to alterations in external environment. The efficiency of plasma membrane perforation was verified for each cell under study by Trypan Blue uptake, which was applied at the end of the experiment. Because the plasma membrane permeability barrier is absent in such cells, volume is determined primarily by volume of its cytoplasm. Furthermore, due to presence of large surface membrane reserves, volume changes are unlikely to be physically restricted by the remaining plasma membrane (22).

Cytoplasm has intrinsic osmosensitivity

An important characteristic of hydrogels is their ability to absorb or release large amounts of water in response to osmolality alteration of the external bathing solution. We tested whether A549 cell cytoplasm shows similar behavior. Indeed, after plasma membrane perforation, variations of external osmolality produced reversible swelling or shrinking of the cytoplasmic gel (see Fig. 3 *a*, *vertical lines 3–4*). In 50% hypotonic solution (~140 mOsm), it further swelled from 2.2- to 3.08- $\pm$ 0.07-fold and shrank to 0.51- $\pm$ 0.01-fold of its initial volume when osmolality of the external solution was increased to ~679 mOsm with mannitol. Results demonstrate that cytoplasm behaves like a hydrogel and has intrinsic osmosensitivity independent of cell surface membrane integrity. Maximal cytoplasm swelling seen with plasma membrane-perforated cells was ~4-fold compared to the initial volume of intact cells. Larger swelling could not be

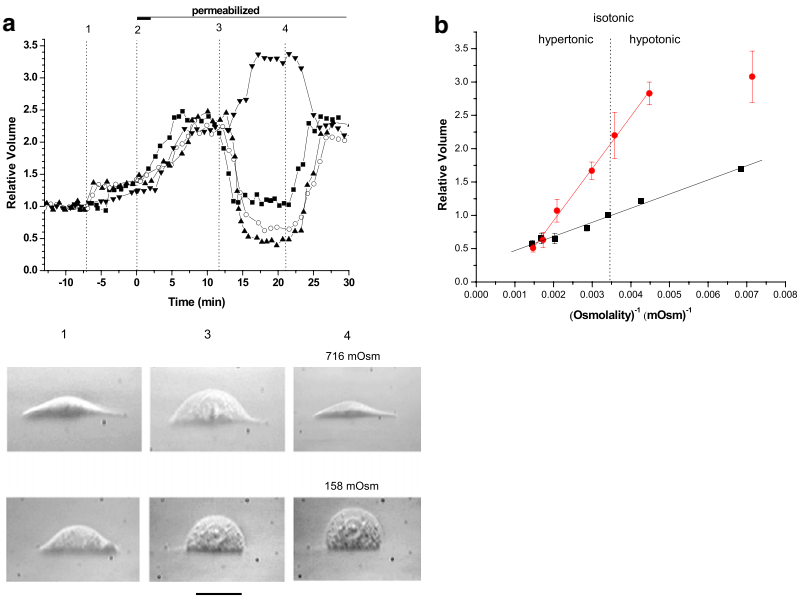

FIGURE 3 (*a*) Time-course of single-cell volume response to membrane perforation and subsequent osmolality changes. Representative traces are shown, each representing a single-cell experiment. Volume changes are relative to initial volume of the cell in PS before membrane permeabilization. The vertical dotted lines indicate: change of external solution from PS to ILS (*1*); plasma membrane permeabilization with digitonin (5 μg/ml, 2 min, denoted by the thick horizontal bar) (*2*); change of external osmolality from isotonic 316 mOsm to (in mOsm): 158 (▼), 516 (■), 616 (○), and 716 (▲) (*3*); return to isotonic conditions (*4*). Below are examples of light microscopic side-view images of two different cells taken sequentially at the time points corresponding to vertical lines *1*, *3*, and *4* as described above. Images were taken via a 20× phase contrast objective (Nikon, LWD, NA 0.4). At *4*, the two cells were exposed to hypertonic (716 mOsm) or hypotonic (158 mOsm0 solutions. The scale bar below corresponds to 20 μm. (*b*) Volume of intact cells (■) and of cytoplasmic gel (●) plotted against reciprocal osmolality. The data points are the average ($\pm$ SE) from 5 to 50 independent experiments. The two straight lines represent a least-square linear regression fitted to the data points in the entire osmolality range tested for intact cells, whereas for permeabilized cells the data point of lowest osmolality was excluded. Corresponding slopes were: 212 $\pm$ 9 mOsm and 782 $\pm$ 24 mOsm and intercepts 0.26 $\pm$ 0.03 and -0.65 ± 0.07.

investigated due to wash-out of cytoplasm content and possible loss of its gel-like consistency in solutions of excessively low osmolality (<140 mOsm). Fig. 3 *b* illustrates the cytoplasm volume observed in external solutions of different osmolalities and compares it to that of intact cells. Assuming a van' t Hoff relationship between volume and inverse osmolality, the linear fit to the 6 points in the range between the 20% hypotonic to the hypertonic osmolality gives the cytoplasm a significant 3.7-fold steeper dependence compared to intact cells. This demonstrates that cytoplasmic gel behaves like a highly sensitive linear osmometer. It deviates from the linear dependence of the ideal osmometer at 50% hypotonicity. This may result, however, from significantly decreased ionic strength of this solution, which was prepared by lowering salt concentration. The high osmosensitivity of cytoplasmic gel is consistent with its extraordinary water-absorbing capacity, a property typical for hydrogels. Interestingly, in the presence of 200 mM mannitol, permeabilized cell volume shrinks back close to that of intact cells, indicating that ~200 mOsm extra osmotic pressure is required to stabilize cell volume. In intact cells, stable steady-state volume is maintained by the plasma membrane, which prevents uncontrolled leakage of osmolytes and reduces intracellular osmotic pressure by energy-dependent ion pumping.

Effect of pH

Swelling of protein-based hydrogels is modulated by pH changes due to alteration of protein surface charge density, electrostatic repulsive forces between neighboring matrix charges and osmotic effects due to altered counterion distribution. We hypothesized that these effects may contribute to pH-dependent volume changes of protein-rich gel-like cytoplasm. Fig. 4 *a* shows that reducing pH of the external solution from 7.4 to 5.0 significantly decreases cytoplasmic volume. The effect was reversible and similar for two different detergents used to permeabilize the plasma membrane. Volume of intact and permeabilized cells reached maximum at pH 7.4 and then declined toward acidic or basic pH values (see Fig. 4 *b*). Interestingly, pH-dependent volume changes of cytoplasm and intact cells were very similar despite a greater than twofold larger initial volume of the cytoplasm caused by Donnan swelling. To determine if such pH dependence is similar in the absence of Donnan swelling, permeabilized cells were examined in solutions of elevated osmolality (with 200 mM mannitol) to reduce their volume back to that observed with intact cells. Fig. 4 *b* illustrates that under these conditions at pH 5, a similar volume reduction occurred as with intact cells. Thus, pH-induced volume changes of intact cells were not different from those of the cytoplasm alone. In intact cells, volume changes may, however, result from pH-induced alteration of transmembrane ionic fluxes and osmotic water movement. To determine the extent of volume changes of intact cells from the latter mechanism, we examined how intracellular pH (pH_i) responds to alterations of extracellular

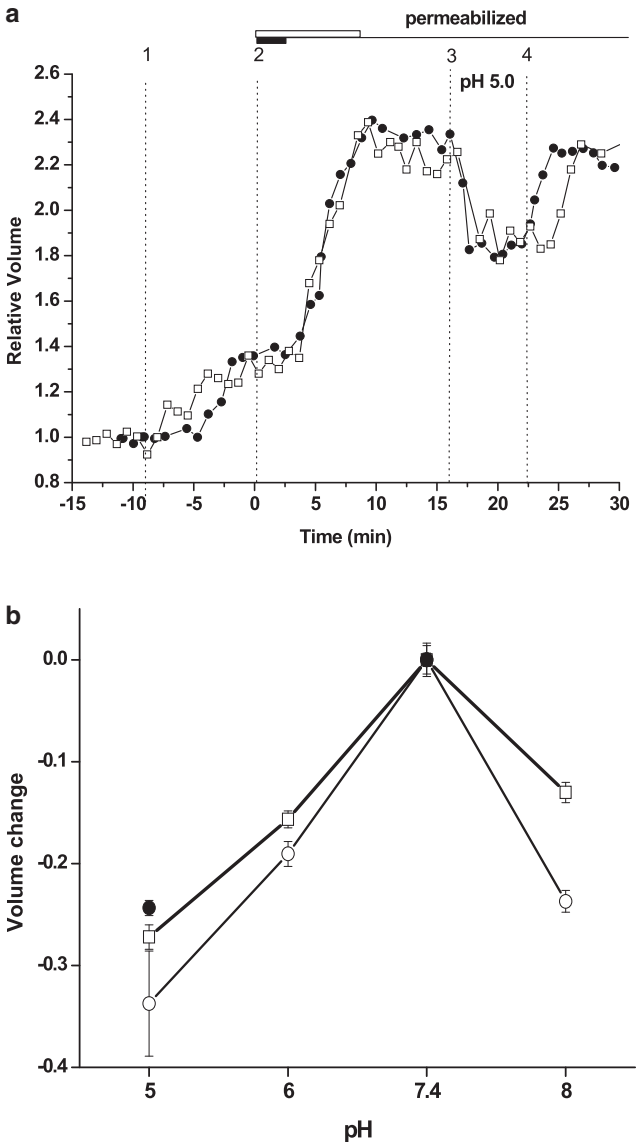

FIGURE 4 (*a*) Time-course of two representative experiments showing effect of external pH changes on permeabilized cell volume. Vertical lines indicate: change of external solution from PS to ILS (*1*); plasma membrane permeabilization with digitonin (5 μg/ml, 2 min) (•) or amphotericin B (8 min, 7.5 μM) (□) (*2*). The thick horizontal bars denote the duration of detergent treatment: white = Amphotericin B, black = digitonin (3); change of external pH from 7.4 to 5.0 (4); return to pH 7.4. (*b*) Comparison of pH-dependent volume changes of permeabilized cells in ILS (○); in ILS + 200 mM mannitol (•) and of intact A549 cells (□). The graph shows the difference between relative volume at pH = X and that observed at pH 7.4 according to the formula: volume change = $V_X/V_0 - V_{7.4}/V_0$, where V_0 = initial volume of intact cell in PS, pH 7.4; $V_{7.4}$ = volume of intact or permeabilized cell in ILS, pH 7.4; and V_X = volume of intact or permeabilzed cell at pH = X. Data points are the average (± SE) from 5 to 50 independent experiments for each condition.

pH. Fig. 5 shows that pH_i of intact cells closely follows that of the extracellular solution, demonstrating that in A549 cells, pH homeostasis mechanisms cannot in the short term compensate for the large pH changes of extracellular solution as cytoplasm is subjected to almost the same pH changes.

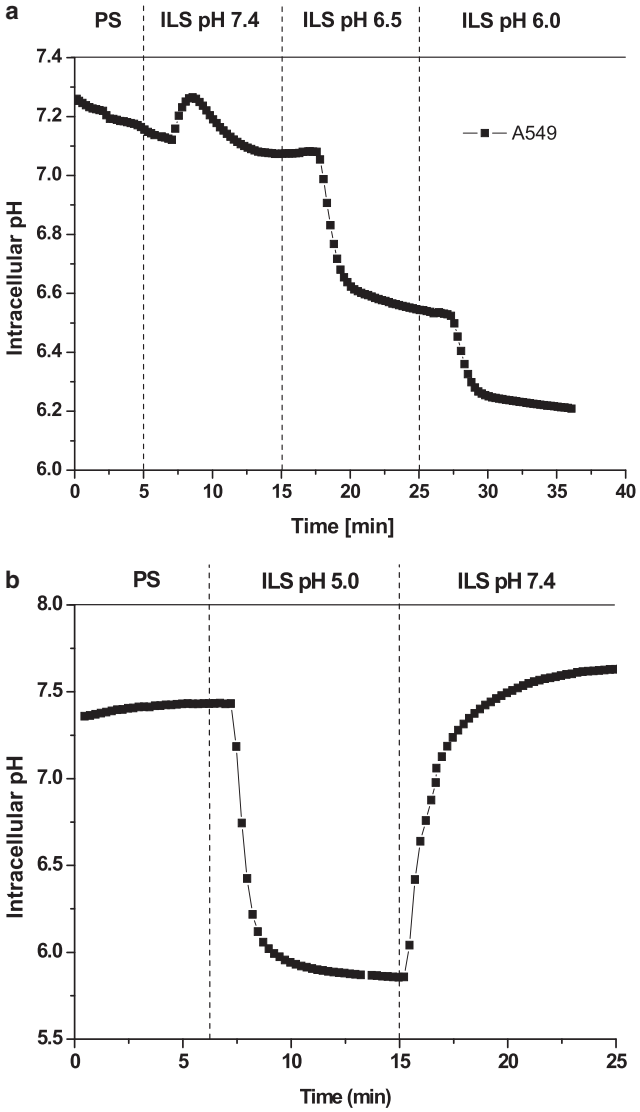

FIGURE 5 Intracellular pH in A549 cells closely follows pH changes of extracellular solution. Time course of pH_i changes after change from extracellular PS to ILS at pH 7.4 and subsequent stepwise reduction of extracellular pH to 6.5 and 6.0 (*a*), and to pH 5 (*b*). Data are representative of $n = 3$ independent experiments. The effect was fully reversible upon returning to extracellular pH of 7.4. All experiments were performed at 37°C; pH_i was measured by BCECF fluorescence imaging (see Methods).

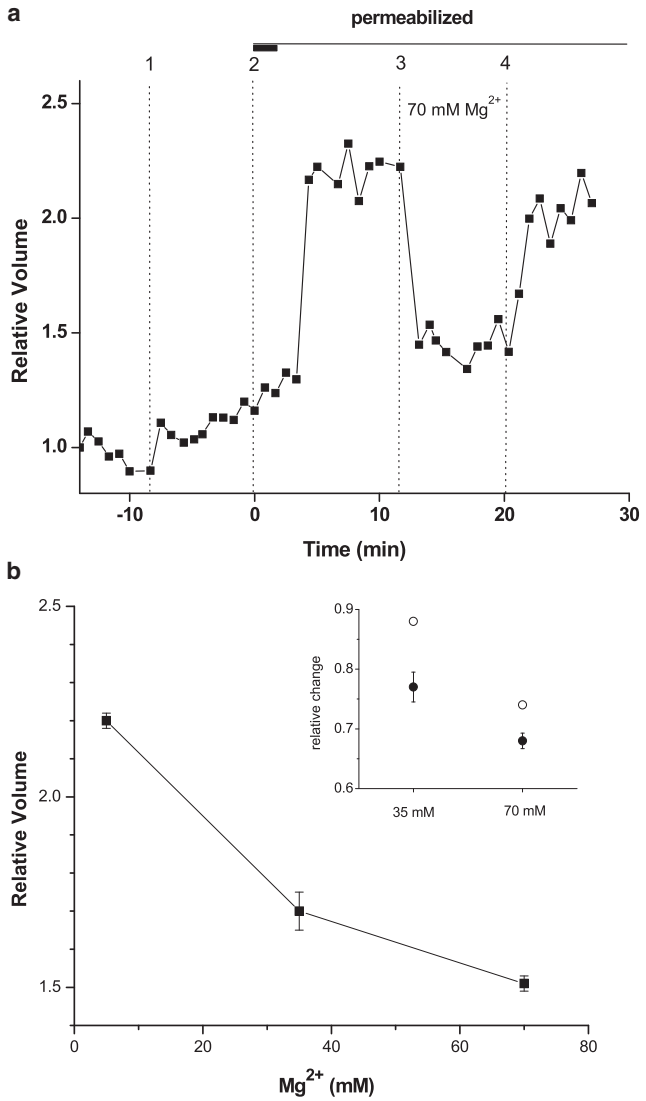

FIGURE 6 Time course of a typical experiment illustrating the volume response to Mg^{2+} elevation. (*a*) Vertical lines indicate: change of external solution from PS to ILS (*1*); plasma membrane permeabilization with digitonin; the thick horizontal bar denotes the duration of detergent treatment (*2*); increased external Mg^{2+} from 5 to 70 mM by isoosmotic replacement of K^+ (*3*); and return to 5 mM Mg^{2+} (*4*). (*b*) Summary of volume responses to different Mg^{2+} levels. Data are mean ± SE of 4–50 independent experiments for each condition. Inset shows experimentally observed relative volume changes (normalized to volume observed with 5 mM Mg^{2+}, (•) induced by different external Mg^{2+} (indicated in mM) and compared to those expected due to reduction of counterion concentration (expressed as relative concentration change) and lower intragel osmotic pressure (○).

Results suggest intrinsic pH-sensitivity of cytoplasm may significantly contribute to volume changes of intact cells during large extracellular pH shifts.

Effect of Mg^{2+}

Swelling capacity of hydrogels, including those with a protein backbone, is known to strongly depend on the surface charges of polymers and is influenced by the ionic strength of the solution and multivalent cations such as Ca^{2+} or Mg^{2+} (8,18,20,26). Therefore, if mammalian cytoplasm is a hydrogel, its volume should be reduced by increasing concentration of divalent cations. We examined the effect of different $MgCl_2$ concentrations on permeabilized cell cytoplasm volume. Fig. 6 *a* reveals isoosmotic elevation of $MgCl_2$ concentration in the external solution from 5 to 70 mM reversibly reduced cytoplasmic volume, and the effects obtained with different $MgCl_2$ concentrations are summarized in Fig. 6 *b*. Shrinkage of cytoplasmic gel in the presence of elevated Mg^{2+} concentrations parallels similar findings with hydrogels and can be attributed to a combination of polymer surface charge screening, ionic crosslinking effects, and

osmotic effects resulting from electroneutral exchange of monovalent K^+ ions by half the number of divalent Mg^{2+}, as required by electroneutrality in the gel matrix (7,11,20). The inset in Fig. 6 *b* shows that observed volume changes are actually larger than expected from ideal osmotic effect of intragel counterion concentration changes alone, suggesting electrostatic forces contribute to cytoplasmic gel volume modulation.

DISCUSSION

The response of cell volume to external environment perturbations has generally been considered an attribute of the plasma membrane. In this study, we show that cytoplasm of mammalian cells behaves as a hydrogel, and, in the absence of plasma membrane barrier, its volume responds reversibly to changes of external osmolality, pH, and the divalent cation concentration. To preserve structural integrity of the fragile cytoplasmic gel, we used single substrate-attached cells whose surface membranes were perforated by gentle treatment with a detergent briefly perfused through the experimental chamber. In most experiments, we used digitonin, a mild nonionic detergent of plant origin. By complexing with membrane cholesterol, digitonin is thought to form pores of 9–10 nm in diameter, allowing molecules of up to 200 kDa to permeate (27). Thus, not only small ions and osmolytes but also mannitol (MW 180) and Trypan Blue (MW 891.8) should readily permeate the digitonin-permeabilized membrane. Because pore formation requires cholesterol, it is anticipated that cholesterol-poor endomembranes such as ER and mitochondria should be much less affected. Considering a relatively low digitonin dose and short exposure, we expect endomembranes to remain largely unaffected. Under these conditions, loss of cellular content is likely limited and cytoplasm gel-like structure is preserved, as indicated by stable volume attained after initial swelling of permeabilized cells. Indeed, release of cellular content after plasma-membrane permeabilization was reported to be much slower than expected for freely diffusing molecules, e.g., mouse L929 cells released only 10–15% of cellular proteins during 30 min permeabilization (1,28). There is evidence that not only proteins but also small ions do not simply leak-out of permeabilized cells. Detergent-treated lens fiber cells (12), kidney epithelial BSC-1 cells (15), and lymphocytes (16) were found to retain much of their protein and K^+ content.

Permeabilization of plasma membrane resulted in a significant 2.3-fold swelling that was similar for all three cell lines tested. One possible interpretation of this swelling involves the Donnan effect, i.e., the fixed negative charges of cytoplasmic proteins attract counterions, which in the absence of compensatory mechanisms lead to increased osmotic pressure, water influx, and cell swelling. It is thought that in intact cells, Na^+,K^+-ATPase-dependent active Na^+ extrusion maintains a steady state in which intracellular Na^+ and, by electroneutrality requirement, Cl^- concentrations are reduced, resulting in osmotic balance and stable cell volume. Inhibition of active Na^+ pumping leads to increased intracellular Na^+ and Cl^- concentration and cell swelling (25). Extent of this swelling varies greatly between different cell types from 30% up to 170% after ouabain inhibition of Na^+,K^+-ATPase (29,30). Similarly, this mechanism of volume stabilization is abolished in permeabilized cells when ions can move freely across plasma membrane leading to a net influx of ions and water into the cytoplasm. The 2.3-fold cytoplasm swelling observed in this study after membrane permeabilization may be counterbalanced by elevating external osmotic pressure by ~200 mOsm. Large swelling was reported for the secretory granule matrix of mast cells and mucins during exocytosis. Gel-forming mucins are tightly packed inside the granules due to low pH and high Ca^{2+} concentration but undergo significant swelling during exocytotic release (31). Mast cell matrix acts as an ion exchanger and swells when native multivalent counterions are exchanged by monovalent cations present in the external bathing solution. This results in increased osmotic pressure and water influx (11). We could speculate that a similar effect, i.e., leakage of native multivalent counterions from the cytoplasm, may be a contributing factor in the initial swelling observed upon membrane permeabilization. However, the nature of such native cytoplasmic counterions remains speculative.

We found that cytoplasm volume responded to variations in external osmolality, which was adjusted by addition of mannitol to the bathing solution. After crossing digitonin-permeabilized membrane, mannitol likely penetrates the bulk of cytoplasm, which should be considered not as solution or solid gel but rather a sponge-like network of cross-linked fibrous structural elements that partitions the intervening liquid into a series of interconnected interstices, channels, or pores, as proposed in studies by Knull and Minton (4) and Shepherd (44). This concept is not new: the early microtrabecular lattice model (15) and more recently the poroelestic cytoplasm model, in which the cytoplasm has been postulated to have two distinct phases, a solid phase of a network; membranes; and particulates; and a fluid phase consisting of water, ions, metabolites, and soluble proteins (32), which are consistent with this view. The poroelestic cytoplasm hypothesis suggested existence of fluid-filled pores of 30–60 nm based on membrane bleb formation and nonequilibration of hydrostatic pressure in blebbing cells (32,33). This is similar to 50 nm pores in actin-rich cytoplasmic domains determined by partition (molecular sieving) of fluorescent tracer (34). Thus, cytoplasm should behave as a sponge-like porous gel in which the fluid-filled pores are readily accessible for osmolytes such as mannitol. By replacing water molecules and reducing its concentration in the cytoplasm fluid phase, mannitol will exert osmotic pressure on the gel phase. Consistent with the gel-like nature of the cytoplasm, we found that osmolality-induced volume changes were 3.7-fold greater compared to intact cells.

Such large volume responses of permeabilized cells in response to osmolality perturbations demonstrate cytoplasm's ability to absorb or release large amounts of water. This property may allow rapid modulation of local fluidity, diffusive processes, and activity of the intracellular environment (35,36). Cytoplasm volume response deviates from a linear dependence in reduced ionic strength 50% hypotonic solution. In contrast, intact cells displayed a linear relationship in the entire osmolality range tested, demonstrating that they behave as perfect though less sensitive osmometers in accordance with numerous earlier studies reviewed (37). The intercept of extrapolated dependence with the ordinate axis is indicative of cellular dry matter and bound water content, which in this study, amounts to ~26 ± 3%. This value is consistent with the reported total protein, carbohydrate, lipid, and nucleic acid content of up to ~30% of tissue wet weight (38), and with ~20% of osmotically unresponsive water content found, e.g., in human erythrocytes (39). Our observations are also consistent with the studies of *Escherichia coli* cytoplasm, where plasmolysis titration experiments in the high-osmolality region showed a linear change of cytoplasmic water volume with inverse external osmolality and found ~0.45 μl/mg dry weight of bound osmotically unresponsive water (40). From these data (see Fig. 4) (40), it is possible to estimate and compare osmotic sensitivity of *E. coli* cytoplasm with that of mammalian cytoplasm examined in our study. For example, to reduce mammalian cytoplasm volume by 50% from that observed under isotonic conditions (~300 mOsm), it was necessary to increase external osmolality by ~597 mOsm for intact cells but by only ~173 mOsm for permeabilized cells (see Fig. 3 *b*). Similar volume reduction required ~506 mOsm in *E.coli*, which compares well with results obtained with intact cells in this study, indicating similar osmosensitivity of both systems in the presence of intact cytoplasmic membrane.

Cytoplasm swelling observed in this study is unlikely to be significantly restrained or limited by the remaining perforated plasma membrane, due to large membrane excess on the surface of A549 cells. We previously reported that A549 and other mammalian cells have huge surface and intracellular membrane reserves of up to ~4-fold their resting surface area. This allows them to swell by 12.9- ± 1.69-fold before the membrane ruptures (22). A large excess of plasma membrane is present on the surface of A549 cells, likely in the form of membrane folds and other irregularities. This reserve alone enables cells to swell up to 4.5-fold without the contribution of endomembrane exocytosis (22).

A bell-shaped relationship between permeabilized cell volume and pH is reminiscent of a pH-dependent swelling curve reported for collagen-based superabsorbent hydrogel (20), indicating that mammalian cytoplasm may share several biophysical properties with such gel. The volume changes were explained by pH-dependent alteration of protein surface charges, electrostatic repulsive forces and degree of charge screening by counterions. At acidic pH, the gel is neutral; but with increasing pH, the carboxyl -COOH groups are converted to $-COO^-$, increasing anion-anion repulsive forces. Anion density in the hydrogel had a maximum at pH 8 when all carboxyl groups were ionized, resulting in high swelling capacity. At higher pH (beyond 8), the increased number of Na^+ ions from the NaOH caused more effective charge screening, reducing anion-anion repulsive forces and hydrogel volume. Similar mechanism may explain pH-dependent behavior of cytoplasm in our experiments, with the exception that K^+ was present as counterion instead of Na^+ and the observed effects were due to net changes of surface charge density on the multiple cytoplasmic polymers, but mainly proteins. Additional effects related to pH-dependent alteration of protein surface charges may involve changes of protein conformation and aggregation and extent of hydration (35). This was also suggested by behavior of serum albumin in dialysis cassettes experiments (19). In intact mammalian cells, swelling is commonly observed upon acidification due to activation of pH_i-regulatory mechanisms. In renal proximal tubules, this involves activation of basolateral NHE1 and Na^+ uptake, which via Na^+,K^+-ATPase is replaced by K^+. The net effect is increase of intracellular ion concentration and cell swelling. In red cells, acidic pH-induced swelling involves both Na^+/H^+ and $HCO3^-/Cl^-$ exchange. This acidity-induced swelling response is opposite to what we found with permeabilized cells, where both acidification or alkalanization reduced cytoplasm volume. However, in taste-receptor cells, acidic stimuli was found to induce cell shrinkage through its effect on the actin cytoskeleton by shifting equilibrium from F-actin to G-actin and activation of basolateral acid-sensitive cation conductance (41). In our experiments, pH-dependent volume changes of cytoplasm were moderate (~12%/pH unit) for both directions of pH changes. Thus, pH sensitivity of cytoplasm may noticeably affect intact cell volume responses only during sudden and large pH_o shifts, which cannot be compensated by cellular pH_i regulatory mechanisms. It may also play a role in smaller uncompensated pH changes, e.g., under pathological conditions where pH_i regulatory mechnisms are defective. Under such conditions, the pH sensitivity of cytoplasmic volume may contribute to diverse effects detected in cells exposed to an acidotic environment in chronic ischemia and other pathological conditions (42), including suppression of oncosis in renal epithelial cells (43).

The hydrogel nature of mammalian cytoplasm is also supported by the effects of Mg^{2+} on cytoplasmic gel volume found in these experiments. Shrinkage in high Mg^{2+} solutions may be explained by a combination of electrostatic and osmotic effects, when Mg^{2+} replaces K^+ in the gel. In these experiments, KCl in the external solution was isoosmoticaly replaced by $MgCl_2$. However, osmotic pressure inside the gel can be reduced due to lower number of counterions required by electroneutrality. A reduced number of counterions causes a decrease in osmotic pressure; water moves out and the gel shrinks. Thus, cytoplasmic gel behaves like an ion

exchanger, where one divalent cation (e.g., Mg^{2+}) replaces two monovalent (e.g., K^{+}) cations, a phenomenon similar to that reported for secretory granule matrix (11). However, as the inset in Fig. 6 *b* shows, the osmotic effect alone could not fully explain the observed Mg^{2+}-induced volume changes, and its contribution is likely overestimated because only a fraction of counterions are osmotically active (7). Thus, there is an important contribution of electrostatic effects, where Mg^{2+} may reduce cytoplasmic gel volume by providing more effective charge screening and by reducing electrostatic repulsive forces in the polyelectrolyte gel. In addition, tighter packing of the cellular matrix could result from ionic crosslinking effect, which involves electrostatic attractive forces between Mg^{2+} and two or more neighboring anionic polymers. Indeed, swelling driven by electrostatic repulsion is thought to be a dominating mechanism of swelling in biological tissues (9).

This study establishes that mammalian cytoplasm shares several biophysical properties with hydrogels. Single cells with their plasma membrane permeability barrier removed swell and shrink depending on ionic conditions, osmolality, and pH, as do nonliving hydrogels. On the one hand, this study fills the gap between whole tissue hydration/dehydration research (12,13). In addition, the vast information on artificial and natural hydrogel properties (7,20), together with results from model systems such as dialysis cassettes filled with natural proteins (19) and other cell types, e.g., plant cells (44), provide a full spectrum of complementary data convincingly supporting that cytoplasm is indeed a gel. This is consistent with the recent realization that an abundance of proteins are significantly unfolded under physiological conditions. Flexible, unstructured polypeptides at high concentrations found in the cytoplasm are expected to cause local cytoplasmic regions to become gel-like (45). The gel-like character of cytoplasm has consequences on cellular behavior. For example, this study reveals that, due to super-swelling capabilities, cytoplasmic volume senses even minute changes in extracellular environment osmolality. This is especially relevant to the mechanism underlying cell volume sensing by eukaryotic cells, which remains unknown despite more than six decades of investigation (46). The results strongly suggest that osmosensitivity of the gel-like cytoplasm, rather than the cytoskeleton and other membrane-bound structures, plays a key role in detecting cell volume perturbations caused by osmolality changes. Due to the extremely sharp dependence of biochemical reactions on macromolecular crowding (38), cytoplasm volume alterations will affect numerous well-documented, volume-dependent cellular responses (37).

In summary, this study reveals that in the absence of a surface membrane permeability barrier, cytoplasm of mammalian cells behave as a hydrogel whose volume reversibly responds to changes in external osmolality, pH, and Mg^{2+} concentration. Cytoplasm's gel-like properties may play a key role in osmosensing and contribute to extracellular pH sensing, and these functions may be complementary to those of the plasma membrane. Undoubtedly, the cell-surface membrane, with its array of ion channels and pumps, plays an active role in preventing Donnan swelling of the cytoplasm and in adjusting optimal cell volume under different environmental conditions. Thus, these findings should help unify the two opposing concepts of the cell viewed as a gel or as a water-filled membrane bag.

This work was supported by grants from the Canadian Institutes of Health Research (to R.G.) and the Natural Sciences and Engineering Research Council of Canada (to R.G. and S.N.O.).

REFERENCES

1. Luby-Phelps, K. 2000. Cytoarchitecture and physical properties of cytoplasm: volume, viscosity, diffusion, intracellular surface area. *Int. Rev. Cytol.* 192:189–221.
2. Leterrier, J. F. 2001. Water and the cytoskeleton. *Cell Mol. Biol.* 47:901–923.
3. Clegg, J. S. 1984. Intracellular water and the cytomatrix: some methods of study and current views. *J. Cell Biol.* 99:167s–171s.
4. Knull, H., and A. P. Minton. 1996. Structure within eukaryotic cytoplasm and its relationship to glycolytic metabolism. *Cell Biochem. Funct.* 14:237–248.
5. Peppas, N. A., Y. Huang, M. Torres-Lugo, J. H. Ward, and J. Zhang. 2000. Physicochemical foundations and structural design of hydrogels in medicine and biology. *Annu. Rev. Biomed. Eng.* 2:9–29.
6. Flory, P. J. 1989. Statistical Mechanics of Chain Molecules. Oxford University Press, New York.
7. Katchalsky, A. 1964. Polyelectrolytes and their biological interactions. *Biophys J.* 4: Suppl-41.
8. Ricka, J., and T. Tanaka. 1984. Swelling of ionic gels - quantitative performance of the Donnan theory. *Macromolecules.* 17:2916–2921.
9. Elliott, G. F., and S. A. Hodson. 1998. Cornea, and the swelling of polyelectrolyte gels of biological interest. *Rep. Prog. Phys.* 61:1325–1365.
10. Brown, A., and R. J. Lasek. 1993. Neurofilaments move apart freely when released from the circumferential constraint of the axonal plasma membrane. *Cell Motil. Cytoskeleton.* 26:313–324.
11. Parpura, V., and J. M. Fernandez. 1996. Atomic force microscopy study of the secretory granule lumen. *Biophys. J.* 71:2356–2366.
12. Cameron, I. L., W. E. Hardman, G. D. Fullerton, A. Miseta, T. Koszegi, et al. 1996. Maintenance of ions, proteins and water in lens fiber cells before and after treatment with non-ionic detergents. *Cell Biol. Int.* 20:127–137.
13. Elliott, G. F., J. M. Goodfellow, and A. E. Woolgar. 1980. Swelling studies of bovine corneal stroma without bounding membranes. *J. Physiol.* 298:453–470.
14. Cameron, I. L., N. J. Short, and G. D. Fullerton. 2008. Characterization of water of hydration fractions in rabbit skeletal muscle with age and time of post-mortem by centrifugal dehydration force and rehydration methods. *Cell Biol. Int.* 32:1337–1343.
15. Schliwa, M., J. van Blerkom, and K. R. Porter. 1981. Stabilization and the cytoplasmic ground substance in detergent-opened cells and a structural and biochemical analysis of its composition. *Proc. Natl. Acad. Sci. USA.* 78:4329–4333.
16. Hazlewood, C. F., and M. Kellermayer. 1988. Ion and water retention by permeabilized cells. *Scanning Microsc.* 2:267–273.
17. Perez-Vilar, J., and R. Mabolo. 2007. Gel-forming mucins. Notions from in vitro studies. *Histol. Histopathol.* 22:455–464.
18. Espinosa, M., G. Noe, C. Troncoso, S. B. Ho, and M. Villalon. 2002. Acidic pH and increasing [Ca(2+)] reduce the swelling of mucins in primary cultures of human cervical cells. *Hum. Reprod.* 17:1964–1972.
19. Cameron, I. L., K. M. Kanal, and G. D. Fullerton. 2006. Role of protein conformation and aggregation in pumping water in and out of a cell. *Cell Biol. Int.* 30:78–85.

20. Pourjavadi, A., K. Feizabadi, and H. Hosseinzadeh. 2006. Synthesis and swelling behavior of a novel protein-based superabsorbent hydrogel composite: collagen-g-poly (sodium acrylate)/kaolin. *J. Polym. Maters.* 23:331–339.

21. Boudreault, F., and R. Grygorczyk. 2004. Evaluation of rapid volume changes of substrate-adherent cells by conventional microscopy 3D imaging. *J. Microsc.* 215:302–312.

22. Groulx, N., F. Boudreault, S. N. Orlov, and R. Grygorczyk. 2006. Membrane reserves and hypotonic cell swelling. *J. Membr. Biol.* 214:43–56.

23. Boudreault, F., and R. Grygorczyk. 2004. Cell swelling-induced ATP release is tightly dependent on intracellular calcium elevations. *J. Physiol.* 561:499–513.

24. Tatur, S., N. Groulx, S. N. Orlov, and R. Grygorczyk. 2007. Ca2+-dependent ATP release from A549 cells involves synergistic autocrine stimulation by co-released uridine nucleotides. *J. Physiol.* 584:419–435.

25. Strange, K. 1989. Ouabain-induced cell swelling in rabbit cortical collecting tubule: NaCl transport by principal cells. *J. Membr. Biol.* 107:249–261.

26. Tibbits, C. W., A. J. MacDougall, and S. G. Ring. 1998. Calcium binding and swelling behaviour of a high methoxyl pectin gel. *Carbohydr. Res.* 310:101–107.

27. Schulz, I. 1990. Permeabilizing cells: some methods and applications for the study of intracellular processes. *Methods Enzymol.* 192:280–300.

28. Clegg, J. S., and S. A. Jackson. 1988. Glycolysis in permeabilized L-929 cells. *Biochem. J.* 255:335–344.

29. Pchejetski, D., S. Taurin, S. S. Der, O. D. Lopina, A. V. Pshezhetsky, et al. 2003. Inhibition of Na+,K+-ATPase by ouabain triggers epithelial cell death independently of inversion of the [Na+]i/[K+]i ratio. *Biochem. Biophys. Res. Commun.* 301:735–744.

30. Rajerison, R. M., M. Faure, and F. Morel. 1988. Involvement of Na and Cl in ouabain-induced cell swelling in thick ascending limb of rat kidney. *Pflugers Arch.* 412:491–496.

31. Perez-Vilar, J. 2007. Mucin granule intraluminal organization. *Am. J. Respir. Cell Mol. Biol.* 36:183–190.

32. Mitchison, T. J., G. T. Charras, and L. Mahadevan. 2008. Implications of a poroelastic cytoplasm for the dynamics of animal cell shape. *Semin. Cell Dev. Biol.* 19:215–223.

33. Charras, G. T., J. C. Yarrow, M. A. Horton, L. Mahadevan, and T. J. Mitchison. 2005. Non-equilibration of hydrostatic pressure in blebbing cells. *Nature.* 435:365–369.

34. Janson, L. W., K. Ragsdale, and K. Luby-Phelps. 1996. Mechanism and size cutoff for steric exclusion from actin-rich cytoplasmic domains. *Biophys. J.* 71:1228–1234.

35. Chaplin, M. 2006. Do we underestimate the importance of water in cell biology? *Nat. Rev. Mol. Cell Biol.* 7:861–866.

36. Wheatley, D. N. 2003. Diffusion, perfusion and the exclusion principles in the structural and functional organization of the living cell: reappraisal of the properties of the 'ground substance'. *J. Exp. Biol.* 206:1955–1961.

37. Lang, F., G. L. Busch, M. Ritter, H. Volkl, S. Waldegger, et al. 1998. Functional significance of cell volume regulatory mechanisms. *Physiol. Rev.* 78:247–306.

38. Minton, A. P. 2001. The influence of macromolecular crowding and macromolecular confinement on biochemical reactions in physiological media. *J. Biol. Chem.* 276:10577–10580.

39. Bogner, P., K. Sipos, A. Ludany, B. Somogyi, and A. Miseta. 2002. Steady-state volumes and metabolism-independent osmotic adaptation in mammalian erythrocytes. *Eur. Biophys. J.* 31:145–152.

40. Cayley, D. S., H. J. Guttman, and M. T. Record Jr. 2000. Biophysical characterization of changes in amounts and activity of Escherichia coli cell and compartment water and turgor pressure in response to osmotic stress. *Biophys. J.* 78:1748–1764.

41. Lyall, V., H. Pasley, T. H. Phan, S. Mummalaneni, G. L. Heck, et al. 2006. Intracellular pH modulates taste receptor cell volume and the phasic part of the chorda tympani response to acids. *J. Gen. Physiol.* 127:15–34.

42. Siesjo, B. K., K. Katsura, and T. Kristian. 1996. Acidosis-related damage. *Adv. Neurol.* 71:209–233.

43. Akimova, O. A., D. Pchejetski, P. Hamet, and S. N. Orlov. 2006. Modest intracellular acidification suppresses death signaling in ouabain-treated cells. *Pflugers Arch.* 451:569–578.

44. Shepherd, V. A. 2006. Coherent domains in the streaming cytoplasm of a giant algal cell. *In* Water and the Cell. Gerald H. Pollack, Ivan L. Cameron, and Denys N. Wheatley, editors. Springer, Dordrecht, The Netherlands. 71–92.

45. Bray, D. 2005. Flexible peptides and cytoplasmic gels. *Genome Biol.* 6:106.

46. Mongin, A. A., and S. N. Orlov. 2001. Mechanism of cell volume regulation and possible nature of the cell volume sensor. *Pathophysiology.* 8:77–88.